Neuron, Volume *91*

Supplemental Information

Real-Time Imaging Reveals Properties of Glutamate-Induced Arc/Arg 3.1 Translation in Neuronal Dendrites

Youn Na, Sungjin Park, Changhee Lee, Dong-Kyu Kim, Joo Min Park, Shanthini Sockanathan, Richard L. Huganir, and Paul F. Worley

Figure S1

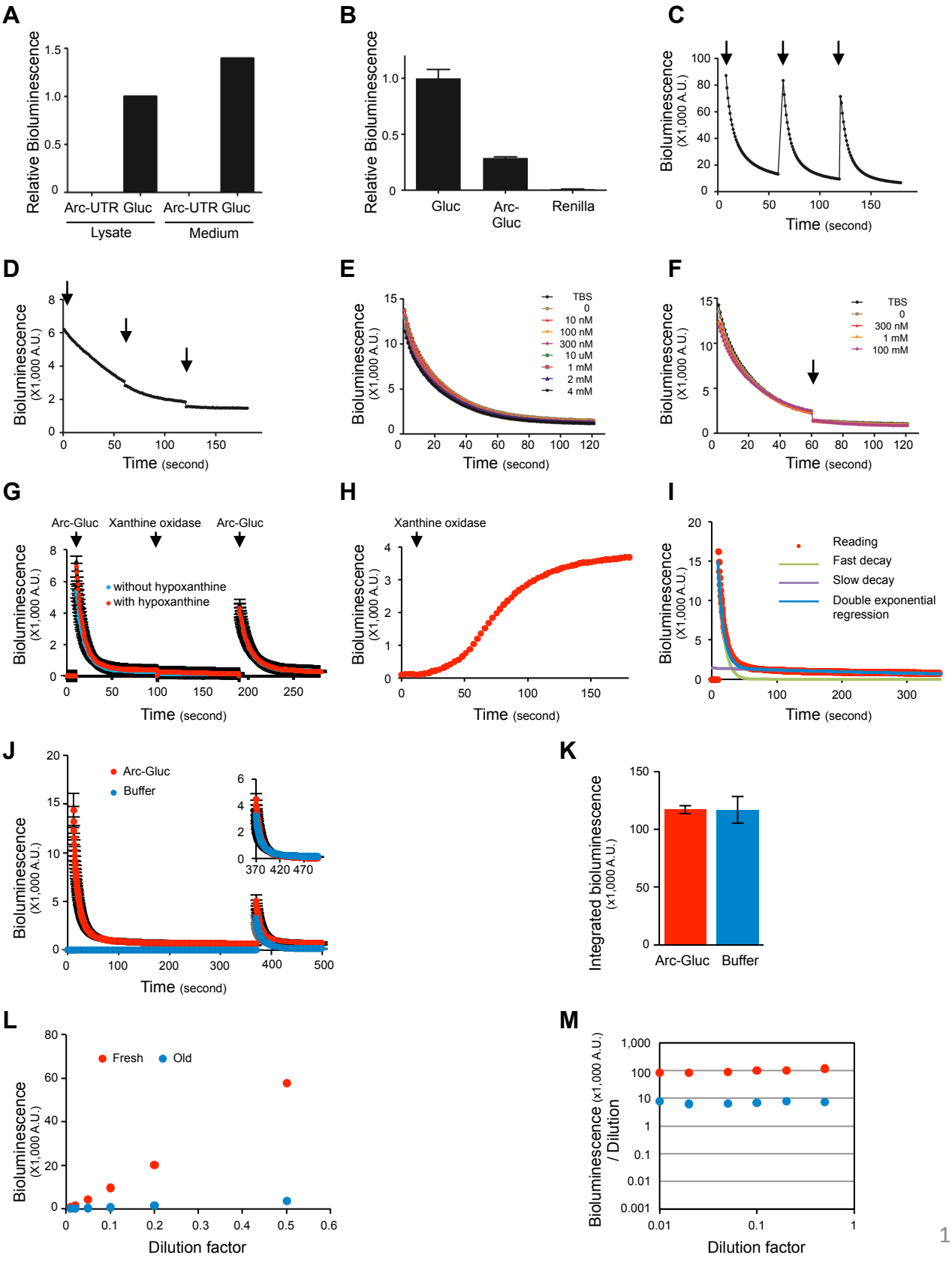
A
Relative Bioluminescence
Arc-UTR Gluc
Arc-UTR Gluc
Lysate
Medium
B
Relative Bioluminescence
Gluc
Arc-Gluc
Renilla
C
Bioluminescence (X1,000 A.U.)
Time (second)
D
Bioluminescence (X1,000 A.U.)
Time (second)
E
Bioluminescence (X1,000 A.U.)
TBS
0
10 nM
100 nM
300 nM
10 uM
1 mM
2 mM
4 mM
Time (second)
F
Bioluminescence (X1,000 A.U.)
TBS
0
300 nM
1 mM
100 mM
Time (second)
G
Arc-Gluc
Xanthine oxidase
Arc-Gluc
without hypoxanthine
with hypoxanthine
Bioluminescence (X1,000 A.U.)
Time (second)
H
Xanthine oxidase
Bioluminescence (X1,000 A.U.)
Time (second)
I
Reading
Fast decay
Slow decay
Double exponential regression
Bioluminescence (X1,000 A.U.)
Time (second)
J
Arc-Gluc
Buffer
Bioluminescence (X1,000 A.U.)
Time (second)
K
Integrated bioluminescence (x1,000 A.U.)
Arc-Gluc
Buffer
L
Fresh
Old
Bioluminescence (X1,000 A.U.)
Dilution factor
M
Bioluminescence (x1,000 A.U.) / Dilution
Dilution factor

Figure S1. Related to Figure 1: Characterization of Gluc luciferase (Gluc) and a fusion protein with Arc (Arc-Gluc). Related to Figure 1. (**A**) Arc does not exhibit luciferase activity. Arc-UTR (Arc ORF with Arc UTR) or Arc-Gluc was transfected to HEK293T cells. The luciferase activities of the lysates and the medium were measured by spectrometry after applying 10 μM Coelenterazine (CTZ). (**B**) Relative luciferase activity. Constructs were transfected to DIV 13 cortical neurons and luciferase activity was measured from cell lysates after applying 40 μM CTZ by spectrometer. The bioluminescence of each was normalized by the bioluminescence of Gluc. Gluc: *Gaussia* luciferase, Renilla: *Renilla* luciferase. (**C**) Flash kinetics of Gluc. CMV-Gluc was transfected to HEK293T cells and medium was collected 2 days later Reaction was initiated by adding 30 μl of Gluc (medium) into 100 μl of 26 μM CTZ. 30 μl of Gluc (Arrows) was added every 56 seconds. Addition of Gluc produced peaks of luciferase signals with fast decay. (**D**) Flash kinetics of Gluc is not due to the depletion of the substrate. Arc-Gluc was transfected to HEK293T cells and lysates were collected 2 days later in passive lysis buffer (Promega). Reaction was initiated by adding 50 μl of 26 μM CTZ to 20 μl of lysates. 50 μl of 26 μM CTZ was added repeatedly every 56 seconds. Additional CTZ did not change the kinetics of luciferase activity. (**E**) Arc-Gluc was transfected to HEK293T cells. The cell lysate (20 μl) was mixed with various concentrations of free Ca^{2+} (80 μl to reach the final concentration indicated) and the reaction was initiated by adding 100 μl of 23 μM CTZ. (**F**) Various concentrations of free Ca^{2+} (80 μl) were added 1 minute after the addition of 100 μl of 23 μM CTZ into 20 μl of enzyme. Additional Ca^{2+} only decreased the signals by diluting the reaction. (**G**) Superoxide or H_2O_2 do not alter bioluminescence of Arc-Gluc. Arc-Gluc was transfected to HEK293T cells and cell lysate was harvested in passive lysis buffer 2 days later. Cell lysate was 1:6 diluted in the Reaction buffer (0.1M Tris-HCl, pH7.5) and 30 μl of Arc-Gluc solution repeatedly injected to 100 μl of substrate solution (30 μM CTZ, with or without 100 μM hypoxanthine (HX) in the reaction buffer) at 10 second and 190 second. Xanthine oxidase (XO, 30 μl of 0.04 U/ml in the reaction buffer) was injected to generate superoxide and H_2O_2 at 100 second (N=3). (**H**) XO produces H_2O_2 in the presence of CTZ. 30 μl of XO (0.04 U/ml in the reaction buffer) was added to 100 μl of Amplex Red substrate solution (30 μM CTZ, 100 μM HX, 0.026 ng/ml of Amplex Red, 0.4 U/ml of HRP in the reaction buffer). H_2O_2, a degraded product of superoxide generated by XO, was measured by Amplex Red fluorescence at 590 nm with an excitation of 530 nm. (**I**) Double exponential regression of Arc-Gluc kinetics shows fast decaying (tau=8.76 seconds) and slow decaying (tau=490 seconds) components. y=15099*exp(-0.1142x)+1436*exp(-0.00204x). R=0.9975. (**J**-**K**) A previous reaction does not affect bioluminescence of fresh enzymes. (**J**) Arc-Gluc was transfected to HEK293T cells and cell lysate was harvested in 1x passive lysis buffer 2 days later. Cell lysate was 1:6 diluted in the Reaction buffer (0.1M Tris-HCl, pH7.5). 100 μl of Arc-Gluc solution (red) or buffer (blue) was injected to 100 μl of substrate solution (60 μM CTZ) at 10 second and 30 μl of Arc-Gluc solution was injected 6 minutes later. Inset: background signal before second addition of Arc-Gluc was subtracted (N=4). (**K**) Integrated bioluminescence of 2^{nd} addition of Arc-Gluc. (**L**-**M**) Dilution of reactants does not affect the bioluminescence per enzyme. Arc-Gluc was transfected to HEK293T cells and cell lysate was harvested in 1x passive lysis buffer 2 days later. Cell lysate was 1:10 diluted in the Reaction buffer. 300 μl of Arc-Gluc was mixed with 900 ml of either buffer (red: fresh) or substrate solution (blue: old) and incubated at room temperature for 1 hour. After incubation, mixtures were further diluted in the Reaction buffer to 1:2, 1:5, 1:10, 1:20, 1:50 and 1:100 fold. Bioluminescence was measured after addition of 150 μl of fresh substrate solution to 50 μl of diluted enzyme. P=0.973 (N=4, two-sample equal variance t-test, 2 tailed, unpaired). (**L**) Bioluminescence is linearly proportional to the amount of enzyme. Fresh enzymes produce higher bioluminescence than reacted enzymes. (**M**) Bioluminescence was divided by a dilution factor to calculate signal/enzyme. Bioluminescence per enzyme remains constant across the dilution, indicating that inhibition of bioluminescence of reacted enzymes is not mediated by reversible inhibitor products. Error bars represent SEM.

Figure S2

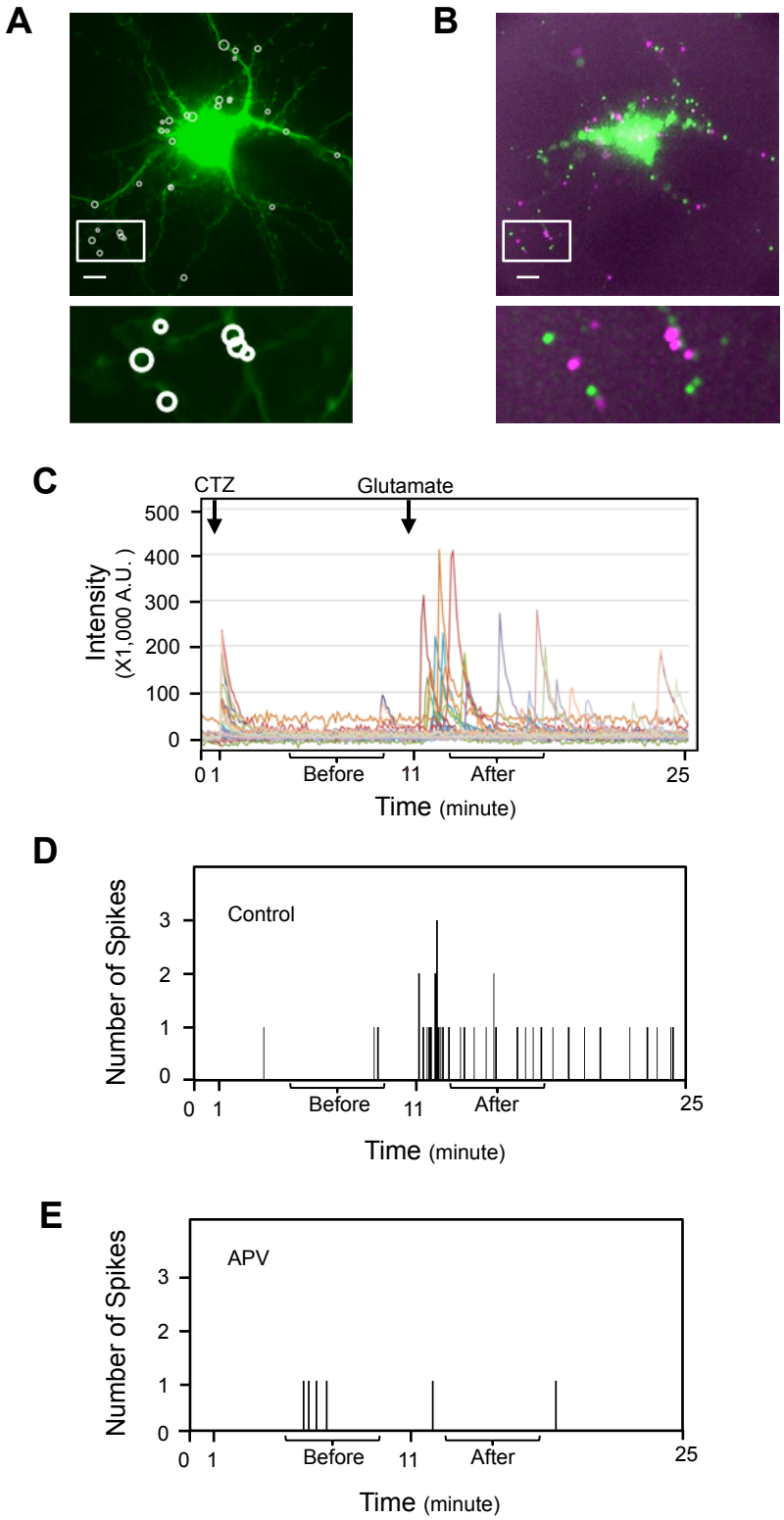
A
B
C
CTZ
Glutamate
Intensity
(X1,000 A.U.)
500
400
300
200
100
0
0 1
Before
11
After
25
Time (minute)
D
Control
Number of Spikes
3
2
1
0
0 1
Before
11
After
25
Time (minute)
E
APV
Number of Spikes
3
2
1
0
0 1
Before
11
After
25
Time (minute)

Figure S2. Related to Figures 2 and 3: Quantification of Arc-Gluc bioluminescence. Related to Figure 2. (**A**) Glutamate-induced Arc-Gluc puncta detected by algorithm were overlaid to EGFP signal. Bottom row shows the magnified pictures from the white square in the upper row. Circle: Arc-Gluc flash at one location. Scale bar: 10 μm. (**B**) Comparing pre-existing Arc-Gluc puncta to glutamate induced Arc-Gluc puncta. Green: after CTZ (pre-existing), Margenta: after glutamate. (**C**) Representative signal traces from one recorded neuron. Each color represents a different luciferase punctum detected by the algorithm. Substrate (CTZ) was added at 1 minute and glutamate was added at 11 minute. Note that due to the different definition of ROI size as well as estimation of background from median intensity level of the entire image (see Experimental Procedures), the initial peak level from pre-existing proteins may be underestimated than manual definition of background ROI. (**D**-**E**) The number of spikes in each frame detected by algorithm was plotted along the recording time. (**D**) Control cell. (**E**) APV pretreated cell.

Figure S3

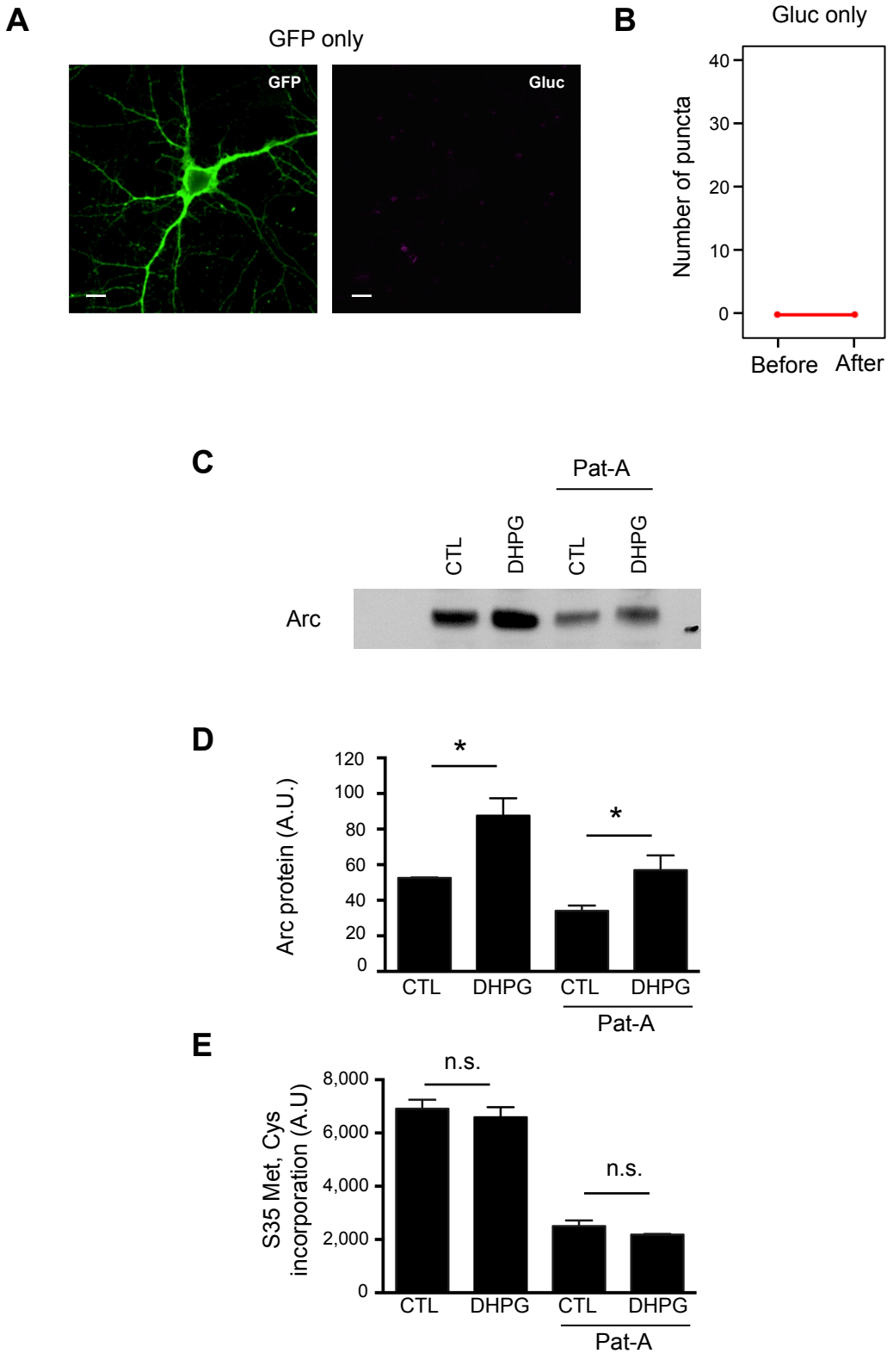
A
GFP only
GFP
Gluc
B
Gluc only
Number of puncta
40
30
20
10
0
Before
After
C
Pat-A
CTL
DHPG
CTL
DHPG
Arc
D
Arc protein (A.U.)
120
100
80
60
40
20
0
*
*
CTL
DHPG
CTL
DHPG
Pat-A
E
S35 Met, Cys incorporation (A.U)
8,000
6,000
4,000
2,000
0
n.s.
n.s.
CTL
DHPG
CTL
DHPG
Pat-A

Figure S3. Related to Figure 4: FISH control and Pateamine A inhibition experiment. Related to Figure 4. (**A**) FlSH (Fluorescence In Situ Hybridization) control. FISH detecting Gluc mRNA was performed after GFP was transiently over-expressed in DIV13-15 cortical neurons. Scale bar: 10 μm. (**B**) The number of dendritic Gluc puncta before (58-97 frames) and after (128-167 frames) glutamate when Gluc was overexpressed. No signal was detected (N=4). (**C**-**E**) Effects of the inhibition of the initiation step of translation on Arc protein level. (**C**) DIV15 cortical neurons were treated with DHPG with or without preincubation of an initiation blocker Peteamine A. DHPG (50 μM, 5 min) induces Arc protein level. Preincubation with Pateamine A (Pat-A:100 nM, 30 min) decreases the basal Arc protein level but does not block the induction of Arc level by DHPG. (**D**) Quantification of Arc protein level by western blot (N=5-6, mean ± SEM). (**E**) Neurons were incubated with ^{35}S Met and Cys (11 mCi/ml) and harvested in RIPA buffer. Proteins were precipitated by 10 TCA and radioactivity were measured by a scintillation counter (N=3-5, mean ± SEM).

Figure S4

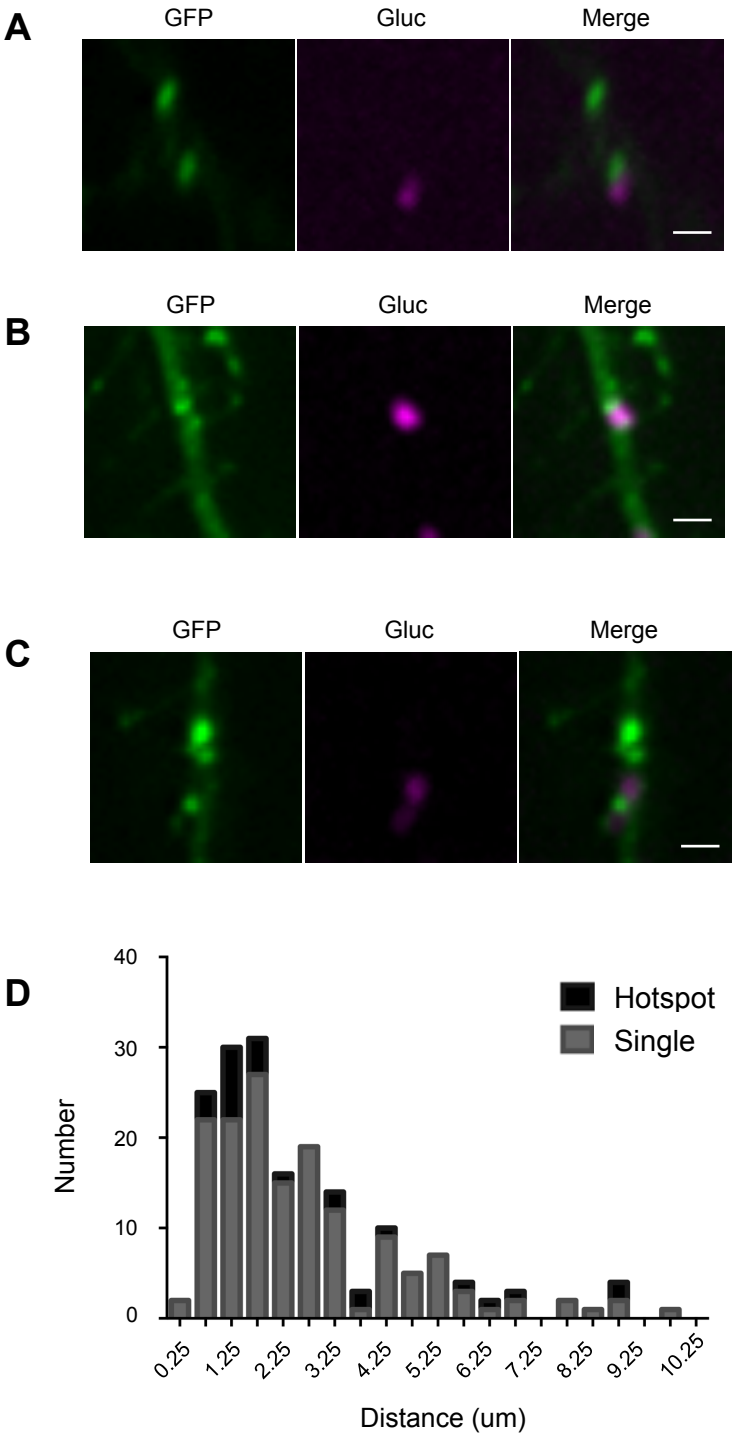
A
GFP
Gluc
Merge
B
GFP
Gluc
Merge
C
GFP
Gluc
Merge
D
Hotspot
Single
Number
40
30
20
10
0
0.25
1.25
2.25
3.25
4.25
5.25
6.25
7.25
8.25
9.25
10.25
Distance (um)

Figure S4. Related to Figure 5: Arc-Gluc is localized in dendrites, not spines. Related to Figure 5. (**A**-**C**) Examples of Arc-Gluc marked by image segmentation algorithm as overlapping with spines based on distance or overlap criteria that by further scrutiny suggest non-co-localization. Scale bar: 2 μm. (**A**) Spine segment and Arc-Gluc elliptic so that the distance is shorter but not overlapping. (**B**) A large, strong Arc-Gluc signal between two spine segments. (**C**) Two Arc-Gluc puncta merged as a hotspot surrounding a spine segment but not located on it. (**D**) Comparison of single translation site verses hotspots in distance between spine and Arc-Gluc centers.

Figure S5

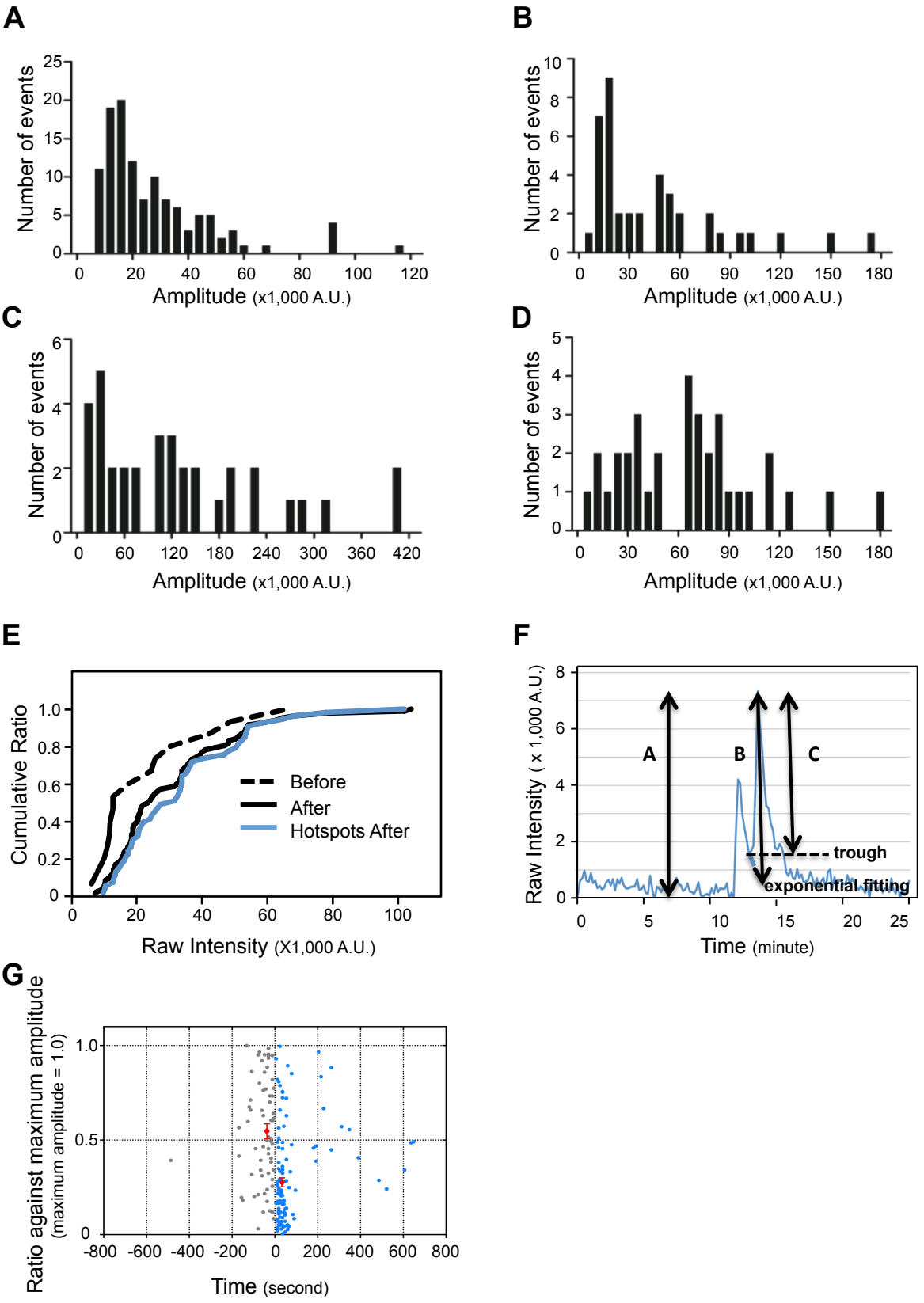
A
Number of events
Amplitude (x1,000 A.U.)
B
Number of events
Amplitude (x1,000 A.U.)
C
Number of events
Amplitude (x1,000 A.U.)
D
Number of events
Amplitude (x1,000 A.U.)
E
Cumulative Ratio
Before
After
Hotspots After
Raw Intensity (X1,000 A.U.)
F
Raw Intensity (x 1,000 A.U.)
A
B
C
trough
exponential fitting
Time (minute)
G
Ratio against maximum amplitude
(maximum amplitude = 1.0)
Time (second)

Figure S5. Related to Figure 7: Characterization of dendritic translation of Arc-Gluc. Related to Figure 7. (**A-D**) Additional examples of the distribution of peak amplitude related to Figure 7A. (**E**) An example of cumulative histogram of amplitude of spikes before and after glutamate treatment. Amplitude histogram of total spikes and spikes at the hotspots are similar. (**F**) A sample trace is shown to illustrate the alternative method of peak intensity estimation. Estimated peak intensity of a peak in hotspot can vary depending on the estimation of baseline. A: intensity estimation of second peak as employed in Figure 7D. If peaks are close together, the tail of the first peak may add to the consecutive peak intensity and result in overestimation. B: The correct estimation of intensity requires subtracting the exponential decay curve from the first peak. However, for many peaks, there was insufficient number of data points to estimate the exponential curve. C: Alternative way to estimate the peak intensity of a consecutive peak is to use the trough between the peaks. This method was used for Figure S5G. This will underestimate the intensity of the second peak. (**G**) The normalized signal intensity of consecutive peaks at hotspots of Figure 7D was redrawn using the trough between peaks as baseline. This shows depression of intensity of second consecutive peaks at hotspots. The two red circles represent the average time interval and normalized amplitude of the second peak succeeding the maximal peak within 100 seconds (time interval from maximum peak=33.2 ± 1.9 seconds, normalized amplitude=0.28 ± 0.02, mean ± SEM, n=99, N=12 cells; time interval before maximum peak=36.8 ± 3.4 seconds, normalized amplitude=0.55 ± 0.04, mean ± SEM, n=53, N=12 cells).

Table S1

	1 event	2 events	3 events	3> events
Cell 1	9	1	0	0
Cell 2	5	0	0	0
Cell 3	27	6	0	0
Cell 4	2	0	0	0
Cell 5	5	1	0	0
Cell 6	11	1	1	3
Cell 7	47	6	6	7
Cell 8	16	1	1	0
Cell 9	11	0	1	0
Cell 10	43	11	2	2
Cell 11	3	2	0	0
Cell 12	28	10	5	2
Cell 13	9	0	0	0
Cell 14	1	0	0	0
Cell 15	2	1	0	0
Cell 16	18	4	0	0
Cell 17	15	5	1	1
Total	**252 (75.7%)**	**49 (14.7%)**	**17 (5.1%)**	**15 (4.5%)**

Table S1. Related to Figure 7: The number of foci showing different number of flashes (presumed translation events) after glutamate treatment (frame 128-250).

SUPPLEMENTAL VIDEOS

Luciferase images were obtained as described in Experimental Procedures. Each frame includes 5 seconds of exposure and 1 second of interval time. Substrate (CTZ) was added at frame 10 and 10 μM of glutamate was added at frame 112. Recording ends at frame 250 (Total 25 minutes). Frames with aberrant noise arising from the camera were deleted for the video presentation.

Video S1. Related to Figure 2: Glutamate induces focal Arc-Gluc bioluminescent flashes. EGFP and Arc-Gluc were co-transfected to cortical neurons.

Video S2. Related to Figure 2: Translation inhibitor blocks glutamate-induced Arc-Gluc bioluminescent flashes. EGFP and Arc-Gluc were transfected to cortical neurons. Translation inhibitor, 100 μM emetine, was added beginning 5 minutes before recording and continuing to the end.

Video S3. Related to Figure 4: Arc ORF is sufficient for glutamate-induced Arc-Gluc bioluminescent flashes.

Video S4. Related to Figure 4: 3myc-Gluc-Arc 51-396 shows glutamate-induced focal bioluminescent flashes.

Video S5. Related to Figure 4: 3myc-Gluc-Arc 51-200 does not show glutamate-induced focal bioluminescent flashes.

Video S6. Related to Figure 7: An example of translation hotspots in dendrites. The peaks of spikes were detected at 124 and 126 frame (white arrow), 115 and 121 frame (yellow arrow), and 127 and 159 frame (red arrow).

SUPPLEMENTAL EXPERIMENTAL PROCEDURES

Cloning

Full length Arc cDNA including 5' and 3' UTR (Genebank: NM_018790) was cloned into EcoRI and XhoI sites of pBluscriptII SK vector. CMV promoter from pEGFP-C1 vector was amplified by PCR with primers flanked by XbaI and EcoRI sites and inserted into the upstream of Arc ORF-UTR sequence. Since the construct contains an EcoRI site between pCMV and Arc 5' UTR to match the transcription start site to endogenous Arc transcript, last 6 bases pCMV were replaced to EcoRI sequence. The expression of the construct was confirmed by western blot. To generate Arc-Gluc fusion construct, PCR product of humanized (codon-optimized) Gluc (NanoLight technology) flanked by 5 glycine linkers was ligated into HincII cleaved mouse Arc ORF-UTR construct. To substitute Arc UTR with g-actin UTR, both 5' and 3' UTR of γ-actin (Genebank: BC023248) were amplified by PCR with flanking primers of Arc ORF. All constructs were confirmed by sequencing.

Reagents and Antibodies

Coelenterazine (CTZ)-native (NanoLight technology) was dissolved in acidic ethanol before the use. For immunocytochemistry, Arc antibody (P.F. Worley, Johns Hopkins University School of Medicine; Maryland; USA Cat# Arc RRID:AB_2313959) and Gluc antibody (Nanolight technology Cat# 401P, RRID:AB_2572411) were used.

Cell Culture and transfection

For primary neuronal culture, cortices from rat embryos were plated onto poly-L-lysine coated coverslips (~50,000 per cm^2) after dissociated in papain and DNase. Neurons were fed twice a week with glial conditioned growth medium. Growth medium contained Neurobasal medium (Gibco) with 1% horse serum and glutamine. Neurons were checked daily to monitor cell growth and process maturation, and only healthy cultures containing neurons showing robust and complex processes without detached cell debris were selected for transfection at DIV 13-15. For the experiment, only healthy GFP+ neurons that showed a uniformed and robust distribution of GFP into distal dendrites without piling or dense clustering were selected. Only neurons that demonstrated these indices of health showed glutamate-induced responses.

In vitro luciferase assay

Gluc constructs were transfected into 6 well plates of HEK293T cells or primary neuronal culture for 1 day. Medium was collected and cells were lysed with 300 µl of Passive Buffer (Promega). Reaction was initiated by adding substrate, CTZ (NanoLight technology) into cell lysates or medium as indicated and luciferase signal was measured by a microplate reader (BioTek). Titration of the concentration of free calcium was calculated using a program supplied from the website below (http://www.stanford.edu/cpatton/maxc.html). Generation of H_2O_2 or superoxide was performed using Amplex Red Xanthine/Xanthine Oxidase Assay Kit as described in the manufacturer's protocol (Invitrogen).

Immunocytochemistry

Cells were fixed with 4% paraformaldehyde, 4% sucrose in phosphate buffered saline (PBS) solution for 20 min and permeabilized with 0.25% Triton X-100 for 10 min. Cells were then blocked with 10% normal goat serum (NGS) for 1 hour and primary antibodies were incubated with neurons at room temperature for 1 hour or at 4 °C for overnight. Cells were washed with PBS and incubated with Alexa Fluor® dyes (1:500; Molecular Probes) for 1 hour at room temperature. After PBS washing, coverslips were mounted with ProLong Gold antifade reagent with DAPI (Invitrogen). For surface labeling, antibodies were incubated without permeabilization.

Time-lapse microscopy

A manual Zeiss AxioObserver microscope (Carl Zeiss MicroImaging) was used with ET525/50 emission filter for GFP fluorescence detection (Chroma Technology) and an EMCCD camera (ImagEMC9100-13, Hamamatsu) for luminescence. Images were acquired using a 63 x 1.4 NA lens (Zeiss). As configured, each CCD pixel corresponded to 0.254 µm diameter of specimen. The camera was maintained at -80 °C during the experiment using a JULABO HF25-ED heating and refrigerated circulator (JD Instruments).

Data analysis for time-lapse images

For manual analysis used in Figure 2, Time Series Analyzer in ImageJ was used. The region of interest (ROI) was selected manually with a constant size during the image. Randomly chosen two areas were used for background. Other Figures and data analysis were generated by an automated analysis using MATLAB. For automated analysis, ROI was defined by providing mask excluding the cell body using ImageJ, and the signal identification method used in analyzing calcium imaging data (Mukamel et al. 2009) (mu=1.0, 200-250 principal components as well as independent components depending on frames taken, standard deviation threshold = 3.0, 8 pixels < area) was adapted to derive the coordinates and area of putative signals (puncta). Puncta from different time points that overlapped significantly were merged. We set the cut-off of defining an active luciferase signal puncta to 6 times

above standard deviation of background noise fluctuation (calculated from individual frames). The time of occurrence of puncta was defined as the time when the puncta had the maximal signal intensity. From each signal trace, the number of distinct spikes was determined. To eliminate any false "blips" arising from potential fluctuation of light intensity unrelated to actual translation events, consecutive peaks were only selected/counted when the peak value was above 3 times the standard deviation of background noise fluctuation (calculated from the actual ROI, before glutamate treatment excluding peak events) from the trough. Aberrant noise arising from the camera was removed based on high signal intensity. Inspection showed a good match of identified puncta by the algorithm to those by manual counting. To estimate the signal intensity of spikes, the value of all pixels of the ROI were added and the median value of each frame excluding the cell body (defined manually by mask) was subtracted for temporal background correction. See also Figure S5F.

Image processing for localization analysis

To determine the location of Arc-Gluc puncta in respect to the position of spines and FMRP, cells were transfected with GFP-PSD95 or GFP-FMRP respectively and the GFP signal was observed before luciferase signal imaging. In addition to intense signal at the spines, GFP-PSD95 produced a weak background signal that marked the dendrites. Image segmentation and classification software Ilastik (Christoph Sommer, 2011) was used to segment the GFP image into PSD, background and dendrite segments. Due to very weak background signal, FMRP images were segmented into FMRP and background only using the same image processing software. An independent operator without knowledge of the analysis derived manually putative dendritic segments based on GFP-FMRP signal and pre-existing Arc-Gluc signal after CTZ. The Euclidian distance to the nearest spine or FMRP segment center was calculated for each Arc-Gluc puncta. Co-localization was defined when the centroid of Arc-Gluc was within PSD95 or FMRP segment. To establish a null distribution of Arc-Gluc puncta, for GFP-PSD95 images, the summed number of pixels of dendrite and Arc-Gluc segments was used.

Statistical analysis

For calculating the null-value for the FMRP and Arc-Gluc co-localization, bootstrapping procedure was performed. From the dendrite segmentation, same number of "null Arc-Gluc puncta" was randomly chosen for each experiment for 50,000 times and the distribution of overlap percentage derived. The bootstrapped p-value for each cell derived by calculating the number of times the overlap frequency was above the experimental value. P-values from six independent experiments were calculated, and the summary p-value was derived using nonparametric Wilcoxon ranked sum test because no assumption on the distribution of p-value (essentially rank) can be made. All data are shown as mean ± S.E.M. and values are presented as means ± 95% confidence interval. No statistical methods were used to pre-determine sample sizes but our sample sizes were similar to those generally employed in the field. We did not perform formal randomization and blinding, although cell cultures were chosen randomly for each experimental group and data were objectively collected and analyzed. For all experiments, the N numbers shown refer to the number of cells used per condition over at least three separate cultures, otherwise mentioned specifically.

SUPPLEMENTAL REFERENCES

Christoph Sommer, C.S., Ullrich K¨othe, Fred A. Hamprecht (2011). ilastik: Interactive Learning and Segmentation

Toolkit. In Eighth IEEE International Symposium on Biomedical Imaging (ISBI), pp. 230-233

Mukamel, E.A., Nimmerjahn, A., and Schnitzer, M.J. (2009). Automated analysis of cellular signals from large-scale calcium imaging data. Neuron 63, 747-760.